Efficiency of High-*n* Rydberg-State Stabilization in Pulsed-Field Ionization Zero-Kinetic-Energy Photoelectron Spectroscopy

J. D. D. Martin and J. W. Hepburn*

Department of Chemistry, Centre for Molecular Beams and Laser Chemistry, University of Waterloo, Waterloo, Ontario, Canada N2L 3G1

C. Alcaraz

LURE, Bât 209D, Centre Universitaire, Paris-Sud, 91405 Orsay, France

Received: March 3, 1997; In Final Form: April 25, 1997[⊗]

To examine the issues concerning Rydberg-state stabilization in pulsed-field ionization zero-kinetic-energy (PFI-ZEKE) photoelectron spectroscopy, spectra at the first and second ionization thresholds of argon have been taken under different ion-density conditions. These provide a contrast between the signals from autoionizing and nonautoionizing Rydberg series. A careful comparison between the PFI-ZEKE spectra and relative partial photoionization cross sections provides the first measurement of the efficiency of stabilization in PFI-ZEKE spectroscopy. This efficiency or quantum yield varies at the second ionization threshold with changing ion density and principal quantum number, introducing ion-density-dependent line-shape distortions. These changes may be ascribed to the competition between stabilization and autoionization of the Rydberg states and its variation with principal quantum number.

1. Introduction

Pulsed-field ionization zero-kinetic-energy (PFI-ZEKE) photoelectron spectroscopy involves the selective detection of electrons field-ionized from optically excited high-*n* Rydberg states ($n = 100-300$).[1,2] By scanning the excitation energy, one can map out the successive ionization thresholds of a neutral species, thereby determining the energy levels of the corresponding ion with significantly improved resolution compared to traditional photoelectron spectroscopy.

In addition to the new spectroscopic information, there has been considerable attention focused on obtaining information concerning the dynamics of the photoionization process from PFI-ZEKE. In particular, the higher resolution has opened up the possibility of comparing rotationally resolved PFI-ZEKE spectra with theoretical partial photoionization cross sections in a number of interesting cases.[3,4] For this comparison to be valid, it is necessary that the detection efficiency of the optically excited Rydberg states be independent of the ionization threshold.

The essence of the PFI-ZEKE technique is the efficient discrimination against prompt photoelectrons from lower ionization thresholds. This is achieved by inserting a time delay between the optical excitation and application of an ionizing electric-field pulse. This delay is typically on the order of 1 μs. To obtain any PFI-ZEKE signal, some fraction of the initially excited Rydberg states must survive this time delay. However, Chupka has pointed out that in certain cases,[5] the experimental observation of a PFI-ZEKE signal is inconsistent with purely field-free, isolated atomic/molecular behavior. The unperturbed Rydberg states may have lifetimes much less than the waiting period between excitation and field ionization.

An illustrative example of this anomaly is the PFI-ZEKE spectra of argon,[6] corresponding to the field ionization of Rydberg states with an electronically excited core (Ar^+, $^2P_{1/2}$). The Rydberg states were excited directly by a single photon from the ground state of the neutral. At excitation energies between the ground state ($^2P_{3/2}$) and the first excited-state ($^2P_{1/2}$) ionization thresholds, it is possible to collect a photoion yield spectrum which shows resonances corresponding to autoionization: excitation of a Rydberg state with a $^2P_{1/2}$ ion core, which subsequently ionizes, ejecting an electron and leaving a ground-state ion ($^2P_{3/2}$). The oscillator strengths for transitions to these series suggest that they are also responsible for excitation of the "ZEKE states" at the excited-state threshold. Fitting the observed low-*n* spectral widths to the well-known n^{-3} scaling law allows one to extrapolate to the high *n* typical of PFI-ZEKE. At 15 cm^{-1} below the threshold ($n = 85$), a lifetime of 6 ns is predicted for the s′ series (the longest lived optically bright series for excitation from the ground state ($^1S_0$) of the neutral). This is inconsistent with the experimental observation of a field ionization signal at 200 ns. PFI-ZEKE spectra have also been taken at the Kr^+, $^2P_{1/2}$ ionization threshold, after much longer time delays.[7,8] In the molecular case, Merkt *et al.*[9] have given a clear exposition of the necessity for a lifetime-lengthening mechanism for PFI-ZEKE spectra of diatomic nitrogen. In this case, predissociation and rotational autoionization are responsible for the decay of the high-*n* Rydberg states. The discrepancy between delay time and extrapolated Rydberg-state lifetimes is common and has been observed for both predissociating and autoionizing Rydberg states of both large and small molecules. It is clear that there must be some mechanism which stabilizes the initially excited low-*l* Rydberg states, such that they survive until field ionization. In particular, the influence of perturbations external to the isolated atom/molecule must be considered.

For high-*n* Rydberg states in the absence of external perturbations, the orbital angular momentum of the Rydberg electron (*l*) is a reasonably good quantum number. Only low-*l* Rydberg series are optically bright in typical excitation schemes. While these low-*l* Rydberg states can decay rapidly, the optically dark high-*l* states decay slowly because of their reduced core penetration. The lifetimes of these states can be comparable with the PFI-ZEKE delay times. An electric field breaks the

* E-mail: hepburn@watsci.uwaterloo.ca.

[⊗] Abstract published in *Advance ACS Abstracts,* July 15, 1997.

S1089-5639(97)00797-4 CCC: $14.00

(almost) spherical symmetry of the electron, ion−core system, causing the Stark mixing of different *l*'s. The stray electric fields typically present in the excitation region are sufficient to cause strong *l* mixing of the high-*n* Rydberg states typical of PFI-ZEKE.[5] Since *l* is no longer a good quantum number for the energy eigenstates, an initially prepared low-*l* state can exhibit a time-dependent behavior, evolving from the initial excitation into a state with mixed-*l* character. As the state gathers more high-*l* character, its autoionization (or predissociation) rate slows. Bixon and Jortner have done a time-independent calculation of the effect of *l* mixing on Ar Rydberg states.[10] Consideration of excitation through a "doorway" state allows them to derive the time-dependent decay of Rydberg states following excitation. These illustrate the rapid loss of Rydberg states due to autoionization immediately following excitation and then a much slower decay rate at longer times after the states are stabilized (*l* mixed). The relative yields of stabilized vs autoionized states depend on both *n* and the strength of the mixing field.

While Stark mixing can lead to an increase in Rydberg-state lifetimes, in some cases, this is not sufficient to explain the presence of the PFI-ZEKE signal. Bixon and Jortner[10] point out that their *l*-mixing calculations underestimate the experimental lifetimes observed by Merkt.[6] It has been suggested that the presence of nearby ions (from prompt ionization) combined with a small dc electric field can break the cylindrical symmetry of the system; i.e., m_l, the projection of orbital angular momentum on an axis, is not a good quantum number of the energy eigenstates[5] (strictly speaking, it is the projection of the total angular momentum of the coupled electron, ion−core system, not m_l, which is the good quantum number of the homogeneous field energy eigenstates). Since high-*l* states have higher m_l degeneracy than low-*l* states, a statistical randomization of the *l* and m_l quantum numbers lowers the decay rates more than *l* mixing alone.[5] These mixing processes vary with *n* so that external perturbations do not affect the low-*n* lifetimes appreciably (where the n^3 scaling law is well obeyed).

Merkt concluded that both *l* and m_l mixing are required for observation of the Ar ($^2P_{1/2}$ ionic core) PFI-ZEKE signal.[6] Merkt and Zare have calculated the ion densities sufficient to cause the necessary cylindrical symmetry breaking.[11] In analogy with the purely *l* mixing studied by Bixon and Jortner,[10] one would expect short time competition between stabilization and autoionization, followed by a much slower decay of the *l* and m_l mixed states. The surrounding ion density will alter the rate of stabilization and, hence, influence the relative yields of stabilized vs autoionized states. There are several experimental results which confirm that the extent of stabilization is influenced by the surrounding ion density. Vrakking and Lee have observed the field ionization signal from Rydberg states of xenon converging on the $^2P_{1/2}$ excited-state core.[12] When they varied the number density of atoms and, hence, the ion density (resulting from excitation leaving $^2P_{3/2}$ ions), the field ionization signal increased with almost the square of the number density. This suggests the competition between autoionization and stabilization. In a set of femtosecond pump−probe experiments, the NRC (Ottawa) group has demonstrated the effects of ion density on the PFI-ZEKE spectra of diatomic iodine.[13,14] By introducing background ions (prior to the femotsecond pump−probe pulses) with an independent laser, they were able to enhance Rydberg-state detection efficiency.

Although the necessity of *l* and m_l mixing has been established for certain specific cases, there remain several important questions, particularly with regard to practical application of the PFI-ZEKE technique. What fraction of initially prepared Rydberg electrons are detected? In other words, what is the "quantum yield"? How is this modified depending on external conditions (ion density, dc fields, etc.)? Does this fraction change at different ionization thresholds (where different Rydberg series are responsible)? If the quantum yield varies from threshold to threshold, this would severely hamper comparisons with theoretical cross sections.

To examine the issues surrounding stabilization in PFI-ZEKE, argon has been studied at its first and second ionization thresholds, leaving $^2P_{3/2}$ and $^2P_{1/2}$ ionic cores, respectively. The first two thresholds provide a nice contrast between PFI-ZEKE signals due to autoionizing ($^2P_{1/2}$ core) and nonautoionizing ($^2P_{3/2}$ core) Rydberg states. Although Rydberg states approaching the $^2P_{3/2}$ threshold can radiatively decay, this is negligible for the time scales and range of *n* considered in this work,[5,15] allowing us to consider the Rydberg states approaching this threshold to be infinitely long-lived. If Rydberg-state stabilization is complete at the $^2P_{1/2}$ threshold, the signals at the two thresholds should be proportional to the relative partial photoionization cross sections at the thresholds. If stabilization is incomplete, the $^2P_{1/2}$ signal would be expected to lose strength compared to the $^2P_{3/2}$ signal.

In essence, comparing these two thresholds allows one to study PFI-ZEKE efficiency, while factoring out trivial aspects, such as electron detection and geometric collection efficiency, flight out of the detection region, etc. These are the same at all ionization thresholds and can be corrected for by a simple multiplicative factor.

2. Apparatus

With the exception of minor changes, primarily to the vacuum system, the apparatus is as described by Kong *et al.*[8,16] The vacuum ultraviolet light (vacuum UV) required for excitation was generated by four-wave sum-frequency mixing in a free jet of krypton.[17,18] Two standard pulsed nanosecond dye lasers were pumped with the second harmonic (SH) and third harmonic (TH) of a Nd:YAG laser with ≈10-ns pulses and a 10-Hz repetition rate. The four-wave mixing process was resonantly enhanced by fixing the frequency-doubled output (ν_1) of the TH-pumped dye laser to a two-photon resonance in Kr ($2\nu_1 =$ 94 093.7 cm^{-1}).[19] The wavelength of the frequency-doubled SH-pumped dye laser (ν_2) was chosen to generate the desired sum frequency ($2\nu_1 + \nu_2$). The ν_1 and ν_2 beams were combined and then focused with a 30-cm lens into a pulsed jet of Kr. The generated vacuum UV was separated from the fundamentals (ν_1 and ν_2) and undesired frequencies ($3\nu_1$, $2\nu_1 - \nu_2$) and refocused by a 1-m normal incidence monochromator (Acton Research Corporation, VM-521-X) into the main experimental region. The monochromator simply acts as a band-pass filter, allowing only the desired high-resolution (≈1 cm^{-1}) vacuum UV to pass. The vacuum UV wavelength was calibrated by a combination of calibrating the two dye laser wavelengths using the optogalvanic effect in Ne and observing the known energy positions of Rydberg states of Ar between the first ($^2P_{3/2}$) and second ($^2P_{1/2}$) ionization thresholds. The system was windowless from generation of the vacuum UV to the experimental region. Differential pumping of the mixing chamber, an intermediate buffer chamber, and the monochromator ensured that mixing gas loading on the main experimental chamber was light.

In the experimental chamber, the vacuum UV intersected a free jet of argon at right angles. The Ar beam was emitted by a pulsed valve (General Valve) with a 1-mm-diameter nozzle located 5.2 cm away from the vacuum UV beam axis. Unlike refs 8 and 16, the beam was unskimmed to allow higher beam

densities to be studied. The vacuum chamber pressure was typically 10^{-7} Torr and rose to 1×10^{-5} Torr with the 10-Hz pulsed argon beam on. The chamber was pumped with a 1000 L/s turbo pump. Thus, the average gas load was 3.3×10^{16} atoms per pulse. Assuming this gas was emitted in 500-μs-long pulses, the average nozzle flow rate during a pulse was 6.6×10^{19} s^{-1}. The formulae of Beijerinck and Verster,[20] as summarized by Miller[21] (his eqs 2.19a−c), may be used to compute the center-line particle flux at the appropriate distance (5.2 cm) from the nozzle opening. At this distance, the argon atoms have essentially reached their terminal speed, computed to be 560 m/s using eq 2.2 of Miller.[21] The particle flux may be divided by this terminal speed to obtain a number density of 3×10^{13} cm^{-3}.

The Ar and vacuum UV beam intersection region was centrally located between two gold mesh electrodes approximately 1.2 cm apart. The electrodes were used to apply a field-ionizing pulse and to draw electrons into an electron spectrometer for the PFI-ZEKE experiments. These electrodes were also used to draw ions into a time-of-flight (TOF) spectrometer in the opposite direction from the electron spectrometer. Microchannel plate detectors are used for both ion and electron detection.

After passing through the Ar beam and the electron and ion spectrometers, the vacuum UV reached a microchannel plate detector, used to monitor the vacuum UV. All three microchannel plate detectors (for vacuum UV, ions and electrons) consisted of two microchannel plates (Galileo Electro-Optics 1330-2500), sandwiched in series separated by 1.8 mm, used in the analog mode. Because of the importance of normalization in the experiments, all detectors were carefully checked for linearity.

After exiting the monochromator, the vacuum UV could be attenuated by the Ar beam before it reaches the microchannel plate detector. In this case, ionization of the Ar would be primarily responsible for absorption. To estimate the size of the effect, the vacuum UV was tuned over an autoionizing resonance 35 cm^{-1} above the first ionization threshold of Ar. Over a 5-cm^{-1} energy range, the ionization cross section jumps from roughly 50 to over 100 Mb.[22] When scanning over this resonance, the reduction in vacuum UV was less than 5% (this upper bound being limited by the signal-to-noise in the vacuum UV detection, as no absorption was observed). This puts an upper bound of 1×10^{-3} Mb^{-1} on the Ar column density. Assuming a standard form for how beam density varies off-axis,[21] this upper limit on the column density is found to be consistent with the estimate of atomic beam density given earlier. Since the total ionization cross section in the energy ranges where PFI-ZEKE spectra were taken in this study is roughly 30 Mb or less, the total attenuation of vacuum UV must have been less than 3%. Hence, operation was under the so-called "thin sample" conditions, and the vacuum UV fluence measured by the microchannel plate detector could be used for normalization.

Although the vacuum UV microchannel plate detector was used throughout the experiment for monitoring and normalization, it was difficult to calibrate for absolute incident photon flux, particularly at the low voltages (and correspondingly low gains) used in the experiment. The typical microchannel plate signals together with a rough estimate of the detector gain suggested that a simple photodiode could be used to determine the vacuum UV fluence per pulse (see, for example, refs 23 and 24). By sliding a copper photodiode in front of the microchannel plate detector, an absolute calibration of the microchannel plate detector was made. It is concluded that the highest photon fluence in this work was roughly 4×10^7 photons per pulse.

Ion density was an important factor in these experiments and must be known for both comparison with theory and other experiments. To determine the ion density, not only is the number of photons per pulse required but also their spatial distribution. Formulae for the spatial properties of the generated four-wave mixed signal as a function of properties of the fundamental beams are given by Lago.[25] After refocusing by the monochromator, astigmatism of the concave grating introduces a vertical spread estimated to be roughly 1 mm (see, for example, ref 24). Defocusing over the 1-cm-long ionization region and diffraction (due to the rulings) also degrade the spot size. Considering these effects, it is estimated that the majority of the vacuum UV was contained within a 1000-μm × 150-μm patch throughout the distance transversed through the detection region. In principle, this could be confirmed by imaging the vacuum UV spot; however, this was not done.

3. Results and Discussion

A. Cross Section Measurements. To compare the PFI-ZEKE spectra at the two ionization thresholds, the relative photoionization cross sections are desired. Before proceeding, it is necessary to establish what is meant by partial photoionization cross sections at energies below the respective ionization threshold for the channel. At the first ($^2P_{3/2}$) ionization threshold, a partial photoionization cross section may be defined below the threshold. In this case, the defined cross section is the same as the total photoabsorption cross section convolved with the excitation bandwidth. This shows a smooth variation over the threshold. This is a consequence of both "continuity of oscillator strength" and the high number of Rydberg states contained within the excitation bandwidth at typical energies below the threshold. Since ions cannot be created below the energetic threshold, the term "photoionization cross section" is somewhat of a misnomer. Perhaps it would be better to refer to the "partial cross section for excitation to the Rydberg pseudocontinuum". However, for brevity, we will use "photoionization cross section".

The situation at the upper threshold is a bit trickier. In this case, $\sigma(^2P_{1/2})$ below the ionization threshold is defined to be the fraction of the photoabsorption cross section which results in excitation of high-n Rydberg states approaching the second ($^2P_{1/2}$) ionization threshold (convolved by the excitation bandwidth). Again, this will smoothly merge with the "proper" $\sigma(^2P_{1/2})$ above the threshold.

These definitions of cross sections are independent of the convolving bandwidth, provided it is much greater than the Rydberg state spacing at the energies of interest (conditions which are normally satisfied in PFI-ZEKE experiments).

It is noted that the extension of partial photoionization cross sections to slightly below their energetic thresholds has been used by Softley and Hudson to compare multichannel quantum defect theory (MQDT) calculated photoionization cross sections with PFI-ZEKE experiments.[26] The agreement between these calculations and previous experimental measurements is excellent.

As noted in the Apparatus Section, the third harmonic of the resonance frequency is also generated in addition to the sum frequency. By adjusting the monochromator, a quick change can be made between sending the sum frequency or third harmonic into the experimental region. By recording light levels and Ar^+ ion signals at these two wavelengths, the ratio of the total cross section at the sum frequency to that at the third

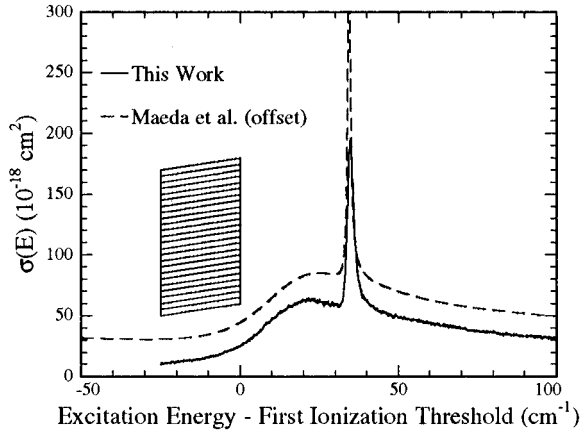

Figure 1. Photoionization cross section of argon near the first ionization threshold. The present results (solid line) are compared with the deconvolved photoabsorption measurements of Maeda *et al.*,[22] which are offset vertically by 20 Mb for clarity (1 Mb = 10^{-18} cm^2). The shaded area represents the energy range for the PFI-ZEKE spectra at the first ionization threshold in this study.

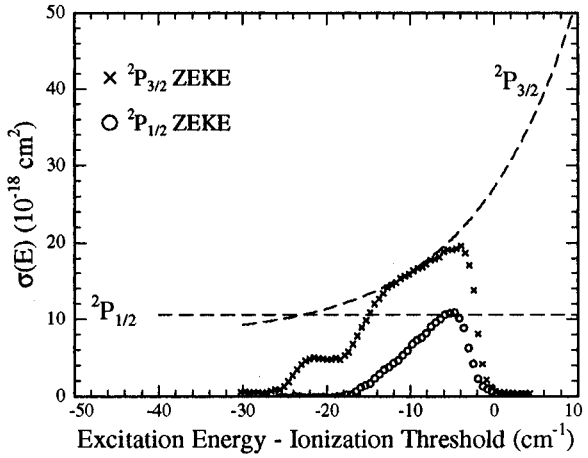

Figure 2. Quantum yield measurements. A comparison between the photoionization cross sections (dotted lines) and PFI-ZEKE spectra at the first ($^2P_{3/2}$) and second ($^2P_{1/2}$) ionization thresholds of argon is plotted as a function of excitation energy relative to the respective ionization thresholds. The two PFI-ZEKE spectra have been scaled vertically by a common factor to allow comparison with the ionization cross sections.

harmonic can be determined. By multiplying the ratio of the relative cross sections by the previously determined photoabsorption cross section at the third-harmonic wavelength,[27] absolute cross sections can be assigned to these measurements. From a different point of view, this is a convenient way of eliminating the need for normalization by molecular beam density, which, while remaining fairly steady on a 1-h time scale, can vary significantly from day to day.

This procedure has been applied to the measurement of photoionization cross sections at both thresholds. At the second ionization threshold, the total photoionization cross section is determined to be 31.0 Mb. This agrees well with a previous measurement of 31 Mb.[27] Two channels contribute to the total ionization cross section: $\sigma(^2P_{1/2})$ and $\sigma(^2P_{3/2})$. Samson *et al.*[28] have measured the branching ratio $\sigma(^2P_{3/2})/\sigma(^2P_{1/2})$ over 25 eV starting at the second IP ($^2P_{1/2}$). It changes surprisingly little from 1.93 over this energy range. Hence, it is assumed that this branching ratio may be applied at the $^2P_{1/2}$ ionization threshold to obtain $\sigma(^2P_{1/2}) = 10.6$ Mb. This cross section has a negligible variation over the range that the PFI-ZEKE spectra cover in this study. However, at the $^2P_{3/2}$ ionization threshold, $\sigma(^2P_{3/2})$ varies strongly, due to the autoionization of Rydberg states converging on the $^2P_{1/2}$ ionization threshold. In fact, two Rydberg states, $3p^5 9d'(^3/_2)_1$ and $3p^5 11s'(^1/_2)_1$, are located 21 and 35 cm^{-1} above the ionization threshold, respectively.[29] Therefore, photoion yield spectra were taken as a function of photon energy in the vicinity of the first ionization threshold. The results are shown in Figure 1.

These determinations of cross sections can be compared with previous studies. In Figure 1, the "deconvolved" photoabsorption spectrum due to Maeda *et al.*[22] has been overlaid. This was generated using the parameters and formulae contained in their paper. In the region where PFI-ZEKE spectra have been taken in this study (shaded in Figure 1), the cross section is roughly 10% higher than that found by Maeda *et al.*[22] However, this is consistent with the estimated uncertainties of both measurements. At the autoionization peak, the disagreement in cross sections is larger, due in part to the finite excitation bandwidth.

B. Quantum Yield. PFI-ZEKE spectra were taken at the first two ionization thresholds of Ar with a pulsed field of 15 V/cm delayed 1 μs after excitation. These two spectra have been normalized by vacuum UV and relative molecular beam density (determined by measurement of the third harmonic ionization signal). As discussed later, the $^2P_{1/2}$ spectrum is specific to a certain set of vacuum UV and molecular beam conditions. To compare the two PFI-ZEKE spectra with their respective partial photoionization cross sections, they have been scaled by a common factor which matches the $^2P_{3/2}$ spectrum to its cross section over the range from 4 to 12 cm^{-1} below threshold. The rescaled spectra and partial photoionization cross sections are shown in Figure 2, plotted as a function of energy below their two respective ionization thresholds at 127 109.5 and 128 541.2 cm^{-1}.[30]

An explanation for the dramatic differences in PFI-ZEKE line shapes at the two ionization thresholds has been put forward by Merkt *et al.*[31] The "shelf-like" structure in the $^2P_{3/2}$ spectrum is due to incomplete field ionization at the red side of the peak. This structure was shown by Merkt *et al.* to scale in energy with varying ionizing field strength. For a certain range of energies below the threshold, the field ionization efficiency is expected to be 100%. So as Figure 2 shows, within the range of 4−12 cm^{-1} below the threshold, the $^2P_{3/2}$ spectrum reflects the energy variation in cross section. At the $^2P_{1/2}$ limit, it is hypothesized by Merkt *et al.* that the same low-*n* states are "filtered" out in the waiting period by spin−orbit autoionization.

It is noted that the $^2P_{1/2}$ PFI-ZEKE spectrum in Figure 2 does in fact approach the limit set by $\sigma(^2P_{1/2})$. In other words, at one particular energy ($\approx$5 cm^{-1} below threshold), the detection efficiency for excited Rydberg states is roughly the same as for the $^2P_{3/2}$ nonautoionizing limit. There are several consequences of this observation.

There are two optically bright Rydberg series which could be responsible for initial excitation: the s and d series. Bixon and Jortner[10] have pointed out, based on a hydrogenic approximation, that the d series should have 20 times the oscillator strength (*n*-independent) of the s series. The actual photoionization yield spectrum between the two limits does seem to support this dramatic difference. As a conservative estimate, Merkt[6] used the field-free s-series lifetimes to show that the unperturbed Rydberg-state lifetimes were too short to be observed. The present results show that the unperturbed lifetimes are in fact significantly smaller than this estimate because it is the optically bright, more quickly autoionizing d series which must be responsible for the bulk of the PFI-ZEKE signal. If the s series were responsible for observation, the $^2P_{1/2}$ spectrum would be much weaker compared with the $^2P_{3/2}$ spectrum.

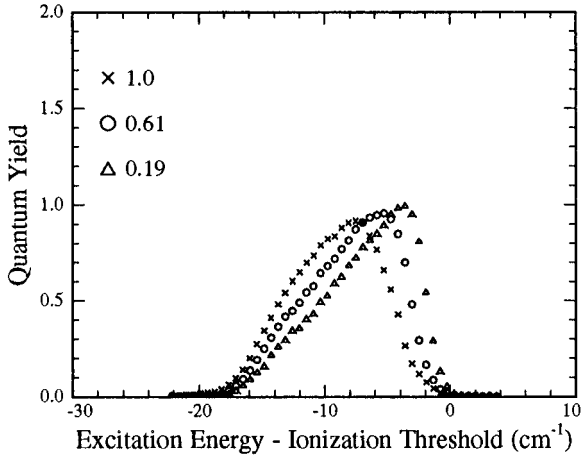

Figure 3. Effects of ion density on the PFI-ZEKE spectra of argon at the $^2P_{1/2}$ limit: high ion densities. These three different PFI-ZEKE spectra were taken at different vacuum UV fluences and normalized by vacuum UV fluence and molecular beam density. The products of vacuum UV and molecular beam density for each of the three traces are contained in the legend (the units are arbitrary but comparable with those in Figure 4). The maximum ion density obtained (1.0 on the arbitrary scale) is approximately equal to 2×10^7 cm^{-3} (see text for details). Note the shifting of the high-energy edge to lower energies with higher ion densities.

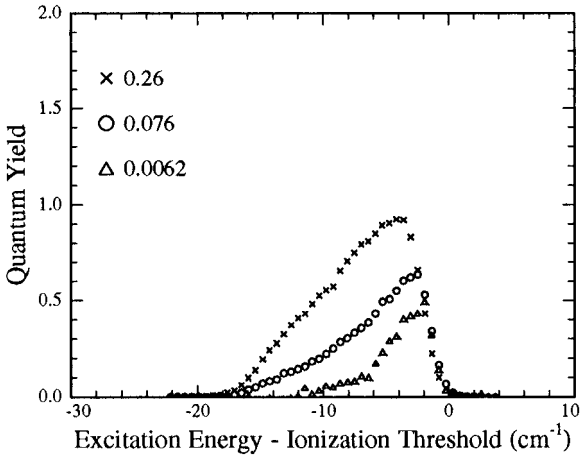

Figure 4. Effects of ion density on the PFI-ZEKE spectra of argon at the $^2P_{1/2}$ limit: low ion densities. These three different PFI-ZEKE spectra were taken at different vacuum UV fluences and normalized by vacuum UV fluence and molecular beam density. The products of vacuum UV and molecular beam density for each of the three traces are contained in the legend (the units are arbitrary but the same as those in Figure 3). Note that the high-energy edge is no longer shifting at these lower ion densities. However, the signal in the center of the peak drops dramatically with lower ion densities.

Unfortunately, these quantum yield experiments do not have the requisite precision to establish whether or not the s series is responsible for any of the PFI-ZEKE signal. The current experiment is not sensitive enough to see the small PFI-ZEKE signal losses that autoionization of the s series would incur.

Despite reaching the maximum expected yield, the $^2P_{1/2}$ PFI-ZEKE spectrum does show a dramatic variation with energy, which is not due to cross section variation (the cross section is flat over this scale). In examining the causes of this variation, it is important to consider two distinct possibilities: (1) The Rydberg states have decayed during the waiting period and, hence, cannot be detected, or (2) while not decaying, a certain fraction of the Rydberg states are not detected in the electric-field ionization. The first type of explanation is contained in the "magic"-zone explanations of PFI-ZEKE line shapes. At a certain critical energy below the threshold, the Rydberg states are no longer sufficiently stabilized in the waiting period and, hence, cannot be detected after the waiting period. This places an upper limit on the width of the PFI-ZEKE line, independent of the strength of the ionizing field. The second possibility is illustrated in the work of Merkt *et al.*,[31] who illustrate that for a certain range of n it is possible to apply multiple successive field ionizing pulses, of the same magnitude and duration, and obtain multiple field ionization signals. In other words, the first and subsequent pulses do not ionize all of the optically prepared, stabilized states. Field ionization efficiency need not be 100%. Any successful explanation of PFI-ZEKE line shapes must consider both of these aspects determining the overall efficiency.

C. Line-Shape Variations with Ion Density. As mentioned, the $^2P_{1/2}$ spectrum shown in Figure 2 was taken under a specific set of vacuum UV and molecular beam conditions. To investigate the possible effects of ion density on the quantum yield, the vacuum UV fluence has been varied by changing the Kr mixing gas density. Measurement of the varying vacuum UV microchannel plate readings should be a direct measurement of how the ion density has changed in the experimental region. This is a distinct advantage of single-photon ionization. There are other possible approaches to varying the ion density in PFI-ZEKE experiments.[12,14,32,33]

Figures 3 and 4 show the effects of varying the vacuum UV and, hence, ion density on the $^2P_{1/2}$ PFI-ZEKE spectra. All of these were taken with a 15 V/cm field-ionizing pulse delayed 1 μs after excitation under approximately the same beam conditions and normalized by the vacuum UV fluence. Based on the quantum yield measurements of the previous section, all spectra were scaled by a common factor, allowing one to interpret the vertical scale as referring to quantum yield. If the PFI-ZEKE spectra showed linear scaling with vacuum UV, these normalized spectra should all be indistinguishable. This is indeed the case at the lower threshold ($^2P_{3/2}$), where the scaling is perfect. The lower threshold verifies detection linearity and the soundness of this procedure. However, as Figures 3 and 4 show, at the upper threshold, the line shapes change dramatically, and the quantum yield drops from 1 with decreasing vacuum UV fluence. The spectra have been divided into two figures, not only for clarity but also because they appear to show two separate phenomena at work.

At the higher ion densities shown in Figure 3, increasing vacuum UV fluence reduced the quantum yield for the high-n portion of the line. Somehow the presence of ions inhibits the ability to see high-n Rydberg states. As discussed in the previous section, experimentally no distinction can be made between destruction of these high-n Rydberg states (by collisional ionization, for example) or a reduced field ionization efficiency. Because this effect appears at the high-n edge of the spectrum, it is believed to be unrelated to autoionization. To test this, a PFI-ZEKE spectra of a mixed Ar, Kr beam was taken at the first ionization threshold of Ar (see Figure 5). Krypton has a lower ionization threshold than argon and, hence, provides a background source of ions. In this case, a virtually identical inhibition of the high-n signal is seen. Zhang *et al.*[33] have noted similar reductions in the high-n PFI-ZEKE signal and have attributed these to ion−Rydberg or Rydberg−Rydberg interactions, as has Merkt.[6]

At the lower ion densities seen in Figure 4, the quantum yield improves at the high-energy side of the peak (it also appears to stop varying with ion density). However, the peak quantum yield drops, and the loss at the low-energy edge is especially dramatic. This behavior is not observed in the $^2P_{3/2}$ spectra with or without Kr present. In other words, the n dependence of the quantum yield varies strongly for states which can autoionize. The fact that the presence of Kr does not effect the low-energy

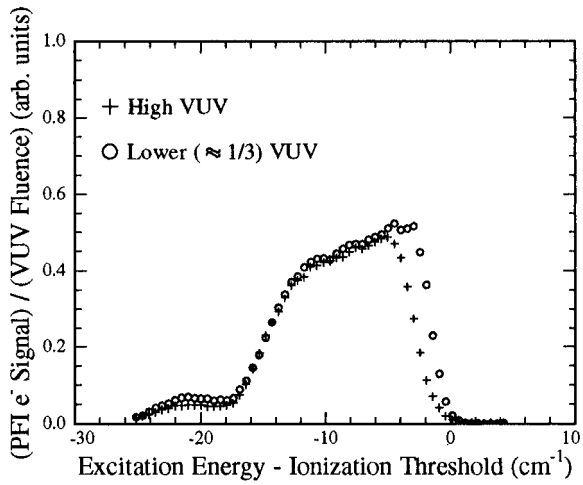

Figure 5. Effects of ion density on the PFI-ZEKE spectra of argon at the $^2P_{3/2}$ limit. The beam contains a mixture of argon and krypton (Kr: Ar ≈ 2). Since Kr has a lower ionization potential than argon, it provides a source of ions at the first ionization threshold of Ar ($^2P_{3/2}$). The two spectra were taken under identical beam conditions with different vacuum UV fluences and then normalized by vacuum UV fluence. Note that the strength of the low-energy "shoulder" is less than in Figure 2. A different pulse generator was used for these spectra, and it is believed that the slew rate of the pulse effects the ionization yield in this region.

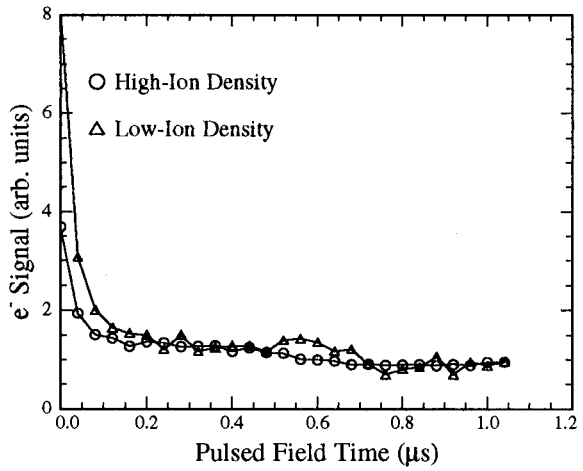

Figure 6. PFI-ZEKE signal decay at 11 cm^{-1} below the $^2P_{1/2}$ ionization threshold of argon. The time between excitation and application of the field ionization pulse is varied while simultaneously scanning the boxcar gate. These have been scaled relative to one another, for comparison of decay behavior from 0.2 to 1 μs.

side of the $^2P_{3/2}$ spectra appreciably at roughly 10 cm^{-1} below the threshold provides strong evidence that possible changes in field ionization efficiency with ion density are not responsible for the variations in quantum yield (from 100%) in the $^2P_{1/2}$ spectra (see Figure 5). With no ion-density influence, it is expected that variations in the field ionization efficiency would only effect the $^2P_{1/2}$ spectra 18 cm^{-1} or further below the threshold (in analogy with the behavior observed at the $^2P_{3/2}$ threshold).

To enable comparison with other experimental conditions and theoretical calculations, the absolute ion densities for the spectra in Figures 3 and 4 are determined using the estimates for atomic beam density, vacuum UV fluence, and spot size estimated in the Apparatus Section. With a photoionization cross section of $\sigma(^2P_{3/2}) = \sigma_{tot} - \sigma(^2P_{1/2}) = 20.4$ Mb at the $^2P_{1/2}$ ionization threshold, the average ion density across the spot at the end of the vacuum UV pulse is computed to be 2×10^7 cm^{-3}. These are the highest ion-density conditions in the experiments (1.0 Arbitrary units in Figure 3).

It is necessary to use caution when interpreting this ion-density estimate. It is clear that spatial variations of vacuum UV and shot-to-shot fluctuations in both the Ar beam intensity and the vacuum UV limit the characterization of ion density with a single average quantity. There are also additional subtleties. For instance, the $\sigma(^2P_{3/2})$ ionization cross section used neglects the contribution from the autoionization of Rydberg states approaching the $^2P_{1/2}$ limit (see the Cross Section Measurements subsection). In fact, as discussed later, ion density is believed to influence the fraction of autoionizing states and, hence, create more ions. Another complication is that Rydberg states are formed and must be stabilized on time scales shorter than the length of the vacuum UV pulse, thus experiencing a time-dependent ion density which varies depending on when the Rydberg states are formed.

D. Lifetime Measurements and a Line-Shape Model. To investigate the reduction in quantum yield at the upper ($^2P_{1/2}$) ionization threshold with different ion densities, an attempt to study the Rydberg states lifetimes was made. By varying the time delay from excitation to pulsed field extraction and the corresponding detection gate, the decay curves as shown in Figure 6 were collected. The large "hump" in the first 0.1 μs is contamination due to prompt electrons. This is determined by comparing these traces to ones taken at energies where no PFI-ZEKE signal is present after a 0.2-μs time delay (by moving to excitation energies several wavenumbers below the field ionization threshold). The decay on the 0.2−1.0 μs time scale was due to flight of the Rydberg atoms from beneath the detector during the waiting period. This was verified by observation of this identical decay at the $^2P_{3/2}$ ionization threshold and a decay rate which could be varied by changing the beam speed. Additionally, the decay was independent of the energy below the threshold (to 15 cm^{-1} below the threshold, which was as far as this was tested). In other words, over the line, the decay was *n*-independent. The two traces shown in Figure 6 were taken under two different ion-density conditions, at 11 cm^{-1} below the ionization threshold, where the quantum yield dropped by 30%. Since the decay behavior is virtually identical on the 0.2−1.0-μs time scale, it is clear that if the reduction in quantum yield is due to Rydberg-state loss, it must occur at short times (<200 ns).

Based on these decay observations, a model for the quantum yield variations with ion density can be formulated (under the assumption that the reduction in quantum yield is due to Rydberg-state decay). Having established that both l and m_l mixing are necessary for stabilization and recalling that m_l mixing can be caused by surrounding ions, it seems reasonable that higher ion densities result in greater stabilization yields. Since signal decay from 0.2 to 1.0 μs is observed to be independent of ion density and n, the n-dependent loss of PFI-ZEKE signal must occur at short times. In fact, because at 11 cm^{-1} below the threshold the d series has a lifetime of 0.2 ns, stabilization must occur on a comparable time scale, if a PFI-ZEKE signal is to be observed. Discussion is simplified by the naive introduction of the "rate of stabilization". For sufficiently high ion density, the stabilization rate could be greater than the autoionization rate, and hence, all states which are excited are stabilized and remain for field ionization. However, if the ion density is reduced, the stabilization rate decreases, and autoionization could become competitive. At low n, the autoionization rate is higher (because of the n^{-3} scaling law), and less states can be stabilized before they autoionize. At higher n, stabilization is more dominant over the slower autoionization rates. Of course, the stabilization rate

also has an n dependence. It is expected to increase with n, thus contributing to the asymmetry at low ion densities. The n dependence of both the stabilization and autoionization processes is a possible explanation of the line-shape distortion dominant in Figure 4 but also present in Figure 3 at low n.

4. Significance and Relationship to Other Works

There appears to be some controversy concerning the role of background ions in PFI-ZEKE spectroscopy. This has been documented by Alt *et al.*,[32] who observe that varying the background ion density has no appreciable effect on the intensity or lifetime of their PFI-ZEKE signal. As they discuss, this is in contrast to the strong effect of ion density found by Vrakking and Lee.[12] Despite this, it is important to note that no contradictory results have been found by different groups working on the same system, suggesting that the comprehensive explanation of the effects of ion density will be subtle.

In fact, as Alt *et al.*[32] pointed out, varying the ion density can have effects on the PFI-ZEKE spectrum other than stabilization. Zavriyev *et al.*[34] mention a "false ZEKE" signal due to a space charge trapping effect. Slow electrons above the threshold remain bound to the ion cloud but are subsequently freed by field ionization, thereby contributing to a false PFI-ZEKE signal. The trapping of slow electrons has been discussed previously in conjunction with the suppression of low energy above the threshold ionization (ATI) electrons.[35] This effect may be considered to be an extreme version of the e^- TOF distortions noticed by Meek *et al.*[36] in the early laser-based TOF photoelectron spectra. In general, we have found that the false PFI-ZEKE signal arising from trapping can be distinguished by observation of the dependence of the PFI-ZEKE signal on excitation energy (particularly if electrons can be observed above a known threshold).

While increasing ion densities can introduce a false PFI-ZEKE signal through space charge trapping at the blue edge of the PFI-ZEKE lines, another phenomenon competes to inhibit the signal at the blue edge. As shown by Zhang *et al.*[33] and in Figure 3 of this work, increasing the ion density inhibits the observation of very high-n Rydberg states. A quantitative explanation of the exact mechanism for this loss has not been made yet.

Another interesting ion-density effect in PFI-ZEKE is the charge-exchange phenomenon.[37] High-n Rydberg states have large cross sections for charge exchange with ions. Smith and Chupka[38] have calculated the electron-transfer rates from Rydberg states to nearby ions under typical experimental conditions. Charge exchange offers an alternative stabilization mechanism for autoionizing Rydberg states. If an electron hops from an excited ionic core to a unexcited core, it will not be able to autoionize. This is clearly a stabilization mechanism which depends on ion density. By collecting mass-analyzed threshold ionization (MATI)[39] spectra, Alt *et al.*[37] were able to observe a field ionization signal arising from one species of ion at the ionization thresholds of another species contained in their molecular beam, a signature of charge exchange. They were able to detect a small but measurable amount of e^- transfer or charge exchange (3% of the parent ion signal), over a time period of a few 100 ns and at an ion density of 5×10^6 cm^{-3}. In the case of stabilization of Rydberg states approaching the $^2P_{1/2}$ ionization threshold of Ar, charge exchange must occur over time periods comparable to the autoionization lifetimes, which are shorter than the time period allowed for exchange in Alt *et al.*'s experiment (where clearly charge exchange plays no role in stabilization). Experimentally, it is difficult to distinguish between l and m_l mixing and charge-exchange stabilization in the presence of small dc fields. They really represent two qualitatively different aspects of the same fundamental phenomena: perturbation of a Rydberg orbital by a nearby charge. However, considering the near 100% quantum yield observed at the high ion densities in this work, it is felt that charge exchange is unlikely to explain the bulk of the stabilization effect in argon.

The extent or efficiency of stabilization is perhaps the key to understanding the apparently disparate results from different experimental groups. In the high-ion-density regime of Figure 3, the actual peak height does not change dramatically with ion density, and thus, one might conclude that there is no ion-density effect, beyond the inhibition of high-n signal as the ion density increases. However, when the efficiency of stabilization is small, varying the ion density can have dramatic effects on the quantum yield, as observed in Figure 4 of this work and by Vrakking and Lee.[12] In fact, recent work by Held *et al.*[40] on benzene has shown that for ion densities of less than 10^5 cm^{-3}, a slow decay of high-n Rydberg states ($n \approx 200$) can be observed, while for higher ion densities no decay can be seen. This possibly explains the earlier benzene results from the same group,[32] where experiments were carried out under higher ion-density conditions and no ion-density effects were reported.

The concept of the efficiency of stabilization is important in the measurement of cross sections. If stabilization is complete for all of the lines in a PFI-ZEKE spectrum, then their relative intensities should be accurate reflections of the corresponding partial photoionization cross sections. If stabilization is incomplete, the different autoionization rates corresponding to Rydberg series converging on different ionization thresholds will distort the possible cross section information available from PFI-ZEKE. Wales *et al.*[41] have hypothesized that the relative strengths of different rotational lines in their PFI-ZEKE spectra of HCl are influenced by variations in the autoionization rates, a nice manifestation of incomplete stabilization.

The different stabilization efficiency regimes were discussed by Vrakking *et al.*[14] They noted that their spectra could be explained by assuming a stabilization efficiency proportional to ion density, which is different from other workers who observe that their stabilization efficiency does not scale with ion density. The present work appears to be the first demonstration of the transition between these two regimes (which involved varying the ion density by more than 2 orders of magnitude).

There is one aspect of stabilization that the present work cannot address, namely, the possibility of intramolecular processes which can occur for large molecules (i.e., benzene). Levine and co-workers (see, for example, ref 42), have considered the rotational−electronic energy exchange between Rydberg electrons and ionic cores that may lead to stabilization. However, the external-field effects discussed in the present paper can be present in large molecular systems and, in fact, have been observed in ZEKE experiments on benzene.[40]

Initial work at the chemical dynamics beamline at the advanced light source (ALS) has demonstrated the applicability of PFI-ZEKE and MATI techniques with broadly tunable, narrow bandwidth vacuum UV.[43,44] There is an exciting potential to apply this apparatus to a variety of interesting threshold photoionization cross-section measurements. However, because of the different repetition rate and intensity of the light source compared to laser-based sources, one can expect to be working under significantly different ion-density conditions. In the MATI experiments on argon, no signal was seen at the $^2P_{1/2}$ ionization threshold, despite the successful observation of the signal at the lower ($^2P_{3/2}$) threshold, and both the

first and second ionization thresholds of neon. We have approximated the field conditions for the ALS MATI experiments (a 0.34 V/cm dc field present during photoexcitation) and find that at the low ion densities (typical of these experiments), the signal is too small to be detected, while increasing the ion density dramatically improves the quantum yield.[45] Over the same range of ion densities with no dc field, the signal always remains detectable. This is consistent with the more recent PFI-ZEKE results from the same group,[44] where under lower dc-field conditions a PFI-ZEKE signal was observed at the Ar $^2P_{1/2}$ ionization threshold (with the same low ion-density conditions as the MATI experiments). Under the quite different experimental conditions of the synchrotron apparatus and other future PFI-ZEKE applications, it is clear that an understanding of the important role of both ion density and dc fields will prove critical in extracting useful cross section information.

Acknowledgment. This work was supported by the Natural Sciences and Engineering Research Council of Canada (NSERC) and by the donors of the Petroleum Research Fund, administered by the American Chemical Society. J. M. thanks NSERC for a graduate scholarship. C. A. thanks NATO for a research fellowship. J. H. acknowledges support from the Canada Council Killam Program.

References and Notes

(1) Reiser, G.; Habenicht, W.; Müller-Dethlefs, K.; Schlag, E. W. *Chem. Phys. Lett.* **1988**, *152*, 119.

(2) Powis, I., Baer, T., Ng, C.-Y., Eds. *High Resolution Laser Photoionization and Photoelectron Studies*; John Wiley and Sons, Ltd.: West Sussex, England, 1995.

(3) Wang, K.; McKoy, V. Rotationally Resolved Photoelectron Spectra at Near-threshold Kinetic Energies. In *High Resolution Laser Photoionization and Photoelectron Studies*; Powis, I., Baer, T., Ng, C.-Y., Eds.; John Wiley and Sons, Ltd.: West Sussex, England, 1995.

(4) Merkt, F.; Softley, T. P. *Int. Rev. Phys. Chem.* **1993**, *12*, 205.

(5) Chupka, W. A. *J. Chem. Phys*. **1993**, *98*, 4520.

(6) Merkt, F. *J. Chem. Phys*. **1994**, *100*, 2623.

(7) Kong, W.; Rodgers, D.; Hepburn, J. W.; Wang, K.; McKoy, V. *J. Chem. Phys.* **1993**, *99*, 3159.

(8) Kong, W. Photoionization Spectroscopy of Small Molecules Using Coherent Extreme Ultraviolet Radiation. Thesis, University of Waterloo, 1993.

(9) Merkt, F.; Mackenzie, S. R.; Softley, T. P. *J. Chem. Phys.* **1995**, *103*, 4509.

(10) Bixon, M.; Jortner, J. *J. Chem. Phys.* **1995**, *103*, 4431.

(11) Merkt, F.; Zare, R. N. *J. Chem. Phys.* **1994**, *101*, 3495.

(12) Vrakking, M. J. J.; Lee, Y. T. *J. Chem. Phys.* **1995**, *102*, 8833.

(13) Fischer, I.; Villeneuve, D. M.; Vrakking, M. J. J.; Stolow, A. *J. Chem. Phys.* **1995**, *102*, 5566.

(14) Vrakking, M. J. J.; Fischer, I.; Villeneuve, D. M.; Stolow, A. *J. Chem. Phys.* **1995**, *103*, 4538.

(15) Chao, S. D.; Lin, S. H.; Selzle, H. L.; Schlag, E. W. *Chem. Phys. Lett.* **1997**, *265*, 445.

(16) Kong, W.; Rodgers, D.; Hepburn, J. W. *J. Chem. Phys.* **1993**, *99*, 8571.

(17) Hilbig, R.; Hilber, G.; Lago, A.; Wolff, B.; Wallenstein, R. *Comments At. Mol. Phys.* **1986**, *18*, 157.

(18) Hepburn, J. W. Generation of Coherent Vacuum Ultraviolet Radiation: Applications to High-Resolution Photoionization and Photoelectron Spectroscopy. In *Laser Techniques in Chemistry*; Myers, A. B., Rizzo, T. R., Eds.; John Wiley and Sons, Ltd.: New York, 1995.

(19) Moore, C. E. *Atomic Energy Levels*; U.S. Government Printing Office: Washington, DC, 1971; Vols. I−III (NSRDS-NBS35).

(20) Beijerinck, H.; Verster, N. *Physica* **1981**, *111C*, 327.

(21) Miller, D. R. Free Jet Sources. In *Atomic and Molecular Beam Methods:* Scoles, G., Ed.; Oxford University: New York, 1988; Vol. 1.

(22) Maeda, K.; Ueda, K.; Ito, K. *J. Phys. B: At. Mol. Opt. Phys.* **1993**, *26*, 1541.

(23) Tonkyn, R. G.; White, M. G. *Rev. Sci. Instrum.* **1989**, *60*, 1245.

(24) Samson, J. A. R. *Techniques of Vacuum Ultraviolet Spectroscopy*; Pied Publications: Lincoln, NE, 1967.

(25) Lago, A. Generation of Coherent Tunable Radiation in the Extreme Ultraviolet by Nonlinear Frequency Mixing of Pulsed Dye Laser Radiation in Rare Gases. Thesis, Universität Bielefeld, 1987.

(26) Softley, T. P.; Hudson, A. J. *J. Chem. Phys.* **1994**, *101*, 923.

(27) Samson, J. A. R. *J. Opt. Soc. Am.* **1964**, *54*, 420.

(28) Samson, J. A. R.; Gardner, J. L.; Starace, A. F. *Phys. Rev. A* **1975**, *12*, 1459.

(29) Yoshino, K. *J. Opt. Soc. Am.* **1970**, *60*, 1220.

(30) Muhlpfordt, A.; Even, U. *J. Chem. Phys*. **1995**, *103*, 4427.

(31) Merkt, F.; Rednall, R. J.; Mackenzie, S. R.; Softley, T. P. *Phys. Rev. Lett.* **1996**, *76*, 3526.

(32) Alt, C.; Scherzer, W. G.; Selzle, H. L.; Schlag, E. W. *Chem. Phys.* **1995**, *240*, 457.

(33) Zhang, X.; Smith, J. M.; Knee, J. L. *J. Chem. Phys.* **1993**, *99*, 3133.

(34) Zavriyev, A.; Fischer, I.; Villeneuve, D. M.; Stolow, A. *Chem. Phys. Lett.* **1995**, *234*, 281.

(35) Crance, M. *J. Phys. B: At. Mol. Opt. Phys*. **1986**, *19*, L671.

(36) Meek, J. T.; Long, S. R.; Reilly, J. P. *J. Phys. Chem.* **1982**, *86*, 2809.

(37) Alt, C.; Scherzer, W. G.; Selzle, H. L.; Schlag, E. W. *Chem. Phys. Lett*. **1994**, *224*, 366.

(38) Smith, J. M.; Chupka, W. A. *J. Chem. Phys.* **1995**, *103*, 3436.

(39) Zhu, L.; Johnson, P. *J. Chem. Phys.* **1991**, *94*, 5769.

(40) Held, A.; Baranov, L. Y.; Selzle, H. L.; Schlag, E. W. The Interactions of a ZEKE Electron with its Ionic Core: An Experimental Measurement. Submitted for publication.

(41) Wales, N. P. L.; Buma, W. J.; de Lange, C. A.; Lefebvre-Brion, H. *J. Chem. Phys.* **1996**, *105*, 5702.

(42) Rabani, E.; Levine, R. D.; Mühlpfordt, A.; Even, U. *J. Chem. Phys.* **1995**, *102*, 1619.

(43) Hsu, C.-W.; Lu, K. T.; Evans, M.; Chen, Y. J.; Ng, C. Y.; Heimann, P. *J. Chem. Phys.* **1996**, *105*, 3950.

(44) Hsu, C.-W.; Evans, M.; Ng, C. Y.; Heimann, P. *Rev. Sci. Instrum.* **1997**, *68*, 1694.

(45) Martin, J. D. D.; Hepburn, J. W. Unpublished results.